Predicting the Optical Performance of Eyes Implanted with IOLs to Correct Spherical Aberration

Juan Tabernero,[1] *Patricia Piers,*[2] *Antonio Benito,*[1] *Manuel Redondo,*[3] *and Pablo Artal*[1]

Purpose. To use powerful modeling techniques for predicting the optical performance of eyes implanted with different types of intraocular lenses (IOLs). This approach will allow performance of "virtual cataract surgery," with different IOL designs that can be used and physical parameters that may occur during actual surgery—in particular, in IOLs that correct spherical aberration.

Methods. A computer model was developed to predict the optical performance of individual eyes after IOL implantation. The approach was validated in a group of patients with eyes implanted with different IOLs. In these patients, corneal wavefront aberrations were calculated from elevations provided by videokeratography. Ocular aberrations were measured with a high-dynamic range Hartmann-Shack wavefront sensor. Misalignments (IOL tilt and decentration) were estimated with a new instrument, based on recording Purkinje images. This model of particular corneal aberrations and IOL parameters (intrinsic optical design details plus geometric location data) was used to estimate the total ocular aberrations after surgery and to compared them with actual aberrations measured directly with the wavefront sensor.

Results. The aberrations of implanted eyes predicted by the individualized optical models were well correlated with the actual aberration measured in each subject. This result indicates that the approach is adequate in evaluating the actual optical performance of different types of lenses. The model allows a large number of "virtual" surgeries to be performed, to test the performance of current or future IOL designs.

Conclusions. A "virtual surgery" approach was designed to predict the optical performance in pseudophakic eyes. In each subject, it was possible to obtain the eye's optical performance with a particular IOL and biometric data after surgery. Specifically, this modeling can be used to evaluate the tolerances to misalignments and depth of focus of IOLs correcting spherical aberration in actual eyes. This approach is quite powerful and is especially applicable to the study of current and future aberration-correction IOL designs. (*Invest Ophthalmol Vis Sci.* 2006;47:4651–4658) DOI:10.1167/iovs.06-0444

A better understanding of the distribution of aberrations in the normal eye[1,2] and the impact of aging[3–5] has resulted in the design of a new generation of IOLs to correct the average corneal spherical aberration (SA).[6,7] New optical and imaging technology permits the combined estimation of both corneal and ocular aberrations. Then, by simple subtraction, it is possible to estimate the internal optical aberration of the eye, mostly corresponding to the lens. Several studies have found that the young lens tends to compensate, at least in part, for the corneal aberrations, but this compensation mechanism is lost with age. Regarding SA, the cornea is clearly positive and changes little with age.[8] However, the young lens has negative SA (allowing for compensation) and evolves toward more positive values with age, losing its compensation ability. Very often, the aging of the human lens also results in optical opacities or cataracts. The current solution to this problem is to implant an artificial lens to restore the optical transparency of the lens (cataract surgery). Some investigators have proposed the use of IOLs to restore not only transparency but also the negative values of SA typically present in younger lenses. These new IOLs were designed with an aspheric anterior surface that induces an amount of SA similar to the average cornea but with the opposite sign (Tecnis TM Z9000 IOL; Advanced Medical Optics [AMO], Santa Ana, CA). The ability of these IOLs to improve the quality of vision has been evaluated both in the laboratory by using adaptive optics[9] and in clinical studies.[10,11] An important issue, already extensively investigated[12–14] but still needing attention and clarification, is the impact of IOL misalignments on optical and visual performance. This question is particularly important in SA-correcting lens design. The aspheric profile of these lenses potentially makes them more sensitive to misalignments than are those lenses with spherical surfaces. In some cases, the benefit of correcting SA could be reduced or even eliminated by the introduction of additional off-axis aberrations.

Traditionally, there have been different approaches to measuring misalignments. Some researchers have used Scheimpflug-based instruments to assess IOL tilt and decentration, but commercially available systems are affected by problems such as corneal magnification that may lead to erroneous results.[15–17] Another traditional method is to use the light reflections at the ocular surfaces (Purkinje images[18]) to estimate ocular alignment.[19–23] We used a new instrument (Tabernero J, et al. *IOVS* 2004;45:ARVO E-Abstract 338; and Tabernero J, et al., manuscript in preparation) based on this approach, for the accurate measurement of IOL tilt and decentration. The combination of measured lenticular tilt and decentration and corneal and IOL geometry allowed us to predict, for the first time in a completely realistic manner, the optical performance in eyes implanted with different types of IOLs. Specifically, we used this modeling, similar to "virtual cataract surgery," to evaluate the tolerances to misalignments and depth of focus for IOLs that correct SA in actual eyes.

From [1]Laboratorio de Óptica, Departamento de Física, Universidad de Murcia, Murcia, Spain; [2]Advanced Medical Optics, Groningen, The Netherlands; and [3]Clínica Ircovision, Cartagena, Murcia, Spain.

Presented in part at the annual meetings of the Association for Research in Vision and Ophthalmology, Fort Lauderdale, Florida, May 2004 and May 2005.

Supported by AMO Groningen BV, Groningen, The Netherlands; and "Ministerio de Educación y Ciencia" Grants BFM2001-0391 and-FIS2004-2153 (PA).

Submitted for publication April 20, 2006; revised May 19, 2006; accepted July 20, 2006.

Disclosure: **J. Tabernero**, None; **P. Piers**, Advanced Medical Optics, Groningen (E); **A. Benito**, None; **M. Redondo**, None; **P. Artal**, Advanced Medical Optics, Groningen (F, C)

The publication costs of this article were defrayed in part by page charge payment. This article must therefore be marked "*advertisement*" in accordance with 18 U.S.C. §1734 solely to indicate this fact.

Corresponding author: Pablo Artal, Laboratorio de Optica, Universidad de Murcia, Campus de Espinardo, 30071 Murcia, Spain; pablo@um.es.

Copyright © Association for Research in Vision and Ophthalmology

Downloaded From: http://jov.arvojournals.org/ on 07/24/2015

METHODS

Subjects

Seven subjects with implanted IOLs were tested in the study. All patients were preoperatively selected with bilateral cataracts and with otherwise healthy eyes. Cataract surgeries were performed by a single surgeon (MR), who performed small-incision surgery, continuous curvilinear capsulorrhexis, and phacoemulsification, followed by implantation of the foldable IOL into the evacuated capsular bag. Measurements were taken 1 month after cataract surgery. A complete set of measurements involved corneal topography to determine corneal aberrations, the measurement of the eye's aberration using a Hartmann-Shack wavefront sensor and IOL misalignment measurements using our custom Purkinje meter system. All clinical examinations, surgeries, and measurements were conducted at Clinica Ircovision (Cartagena, Murcia, Spain). All the subjects were measured with their pupils pharmacologically dilated. Practices and research adhered to the tenets of the Declaration of Helsinki. Informed consent was obtained from each subject after explanation of the nature and possible consequences of the procedures.

The IOLs implanted were the Tecnis TM Z9000 (AMO; four subjects) and the CeeOn TM 911A (AMO ; three subjects). Both lenses are foldable, made from high refractive index silicone (n = 1.458), and have a 6-mm optical zone. The CeeOn TM is a biconvex lens with spherical surfaces. This conventional lens induces a positive SA that increases with lens optical power (Fig. 1). Because corneal SA is normally positive, implanting this lens should generate a significant amount of ocular SA. The Tecnis TM lens has a modified aspheric front surface designed to generate a negative SA (constant with lens power) to compensate for corneal positive SA. This should result in a significant reduction of ocular SA. Spherical aberration for both lenses for a 5-mm pupil as a function of lens power is shown in Figure 1.

Instruments and Measurements

The wave aberration of the cornea was estimated from elevation data obtained by a corneal topographer by performing a ray-tracing procedure through the corneal surface derived from corneal elevations at a sample of points obtained with a Placido-based corneal topographer (Atlas; Carl Zeiss Meditec, Dublin, CA). From the corneal elevations, an analytical expression for the corneal surface was obtained by fitting the sample data to a Zernike polynomial representation. An optical design software package (Zemax Development Corp., San Diego, CA) was used to perform ray-tracing through this surface and calculate the aberrations associated with the corneal surface. This is a procedure that was slightly modified from a similar methodology that described elsewhere,[24] providing similar results. All calculations presented in this study are predicated on a 5-mm pupil diameter. The average corneal heights of three measurements for each subject were used as the nominal value. The corneal aberration maps were centered on the pupil using the distance of the pupil center from the corneal reflex given by the topographer.

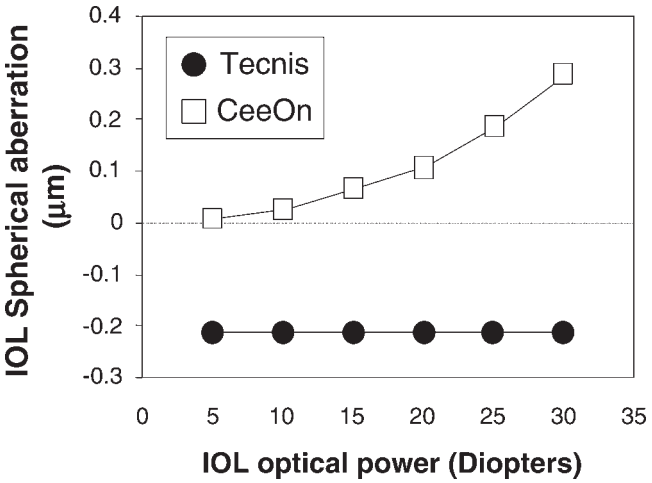

FIGURE 1. Theoretical SA (Z, 4.0) for the two lens designs as a function of their power (5-mm pupil diameter) when they are inserted into the same pseudophakic eye model. These values are calculated by subtracting the corneal SA from the total SA of the eye model for each different IOL power.

We measured the ocular wavefront aberration by using our own research prototype near-infrared Hartmann-Shack wavefront sensor adapted to the clinical environment. This system, described elsewhere,[25] consists of a microlens array, conjugate with the eye's pupil, and a camera placed at its focal plane. If a plane wavefront reaches the microlens array, the camera records a perfectly regular mosaic of spots. However, if a distorted (i.e., aberrated) wavefront reaches the sensor, the pattern of spots is irregular. The displacement of each spot is proportional to the derivative of the wavefront over each microlens area. From the images of the spots, the ocular wave aberration is computed and expressed as a Zernike polynomial expansion. It is a robust system with more than 220 microlenses over a 5-mm pupil area and has a high dynamic range, allowing for the measurement of large aberrations with sufficient accuracy.

IOL tilt and IOL decentration were estimated as well with an instrument we developed based on recording the Purkinje images of a semicircular ring of infrared LEDs for several well-defined fixation positions. This is an improved version of the clinical method proposed by Guyton et al.[26] The technical details of this instrument have been discussed elsewhere (Tabernera J, et al. *IOVS* 2004;45:ARVO E-Abstract 338; and Tabernero J, et al., manuscript in preparation). In summary, the subject fixates sequentially at nine different angular locations. These fixations points are distributed as shown in Figure 2 (marked as fixation LEDs). The more peripheral points subtend an angle of 5° with respect to the central stimulus. An image of the anterior eye containing Purkinje images (first, third, and fourth) is recorded at each fixation position, and the distance from each reflection to the center of the pupil is obtained. These distances are plotted as a function of the angular fixation. From these plots, by linear interpolation (or extrapolation, depending on the subject) we determined the fixation angle where the third and fourth Purkinje images overlap and then, from the distance of this overlapping point (it locates the IOL optical axis) to the entrance pupil center, we estimated decentration of the IOLs. Considering the fact that we know the angle of fixation with respect to a central stimulus at each foveal target, IOL tilt can be calculated. We can refer to this tilt to two ocular axes: the pupillary axis and the line of sight.

In each subject, measurements of axial length and axial intraocular lens position were performed with a conventional ultrasound system.

Computer Modeling: Virtual Optical Surgery

The corneal surface was incorporated in the computer model from the corneal elevation data fit to an eighth-order Zernike expansion by using a least-squares fitting routine. A rectangular Cartesian grid of points from this corneal surface was calculated to serve as an adequate input to the ray-tracing optical software (Zemax Development Corp.). Once into the ray-tracing model, the corneal surface was decenterd relative to the pupil center by those values obtained from the corneal topographer. Details of the IOL geometry and refractive index for both types of lenses were provided by AMO and incorporated into the model. IOL tilt and decentration in each subject were measured after the surgery according to our Purkinje meter system and then incorporated into the calculations together with the IOL's axial position and ocular axial length. The resultant optical models are three personalized eye surface representations (one surface cornea and the intraocular lens). The refractive index used for the aqueous (between the cornea and IOL) was 1.3375 and for the vitreous, 1.336.

Downloaded From: http://jov.arvojournals.org/ on 07/24/2015

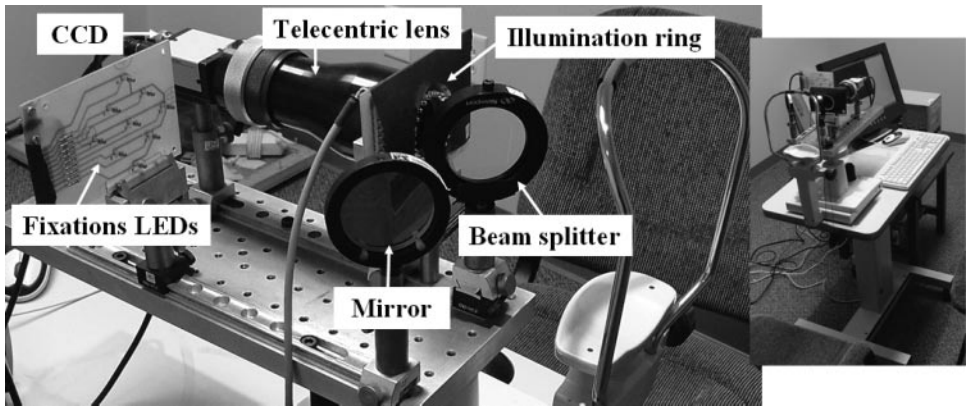

FIGURE 2. Two different views of the experimental system used to measure IOL misalignments.

Once all the experimental data were incorporated into the computer model, we were able to predict the postoperative ocular aberrations for each subject. This prediction, called virtual optical surgery, was compared with the actual measured aberration after the surgery with our Hartmann-Shack wavefront sensor. Figure 3 shows a schematic view of the complete customized procedure, showing actual results from one subject as an example.

This procedure is a powerful way to predict the potential optical quality that would result after surgery for any type of IOL. In this study, we applied this modeling to evaluate the performance of IOLs correcting SA by using actual biometric data from subjects. We can investigate how the eye's optical quality changes when IOL tilt and decentration are continuously modified in the model. In addition, we can also realistically quantify how the optical performance would have been affected if a different IOL had been implanted in a subject. For each individual eye model we can calculate its optical quality with the IOL truly implanted and then exchange the IOL to compare the resultant optical quality.

To investigate the relative optical performance of the two different IOLs analyzed in this study, we defined a parameter (improvement fraction, equation 1) in terms of the radially averaged modulation transfer function (MTF) at a given spatial frequency.

$$\mathrm{IF}(f) = \frac{\mathrm{RadialMTF}_{\mathrm{Tecnis}}(f) - \mathrm{RadialMTF}_{\mathrm{CeeOn}}(f)}{\mathrm{RadialMTF}_{\mathrm{CeeOn}}(f)} \times 100. \qquad (1)$$

A positive value of this parameter means that the Tecnis TM lens (i.e., correcting SA) performs better than the CeeOn TM IOL; while a negative value means the opposite. This parameter was also calculated as a function of possible decentration and tilt of the IOLs.

Depth of focus could also be affecting the relative optical performance of both IOLs. To evaluate this factor, a metric, the volume of the square PSF, was calculated as a function of the image plane axial position (Z).

$$\mathrm{DoF\_}metric(Z) = [\int \mathrm{PSF}^2(x, y)dxdy](Z). \qquad (2)$$

The integral was evaluated numerically using a simple trapezoidal rule. The square PSF has the effect of enhanced relevant peaks of the PSF with respect to lower noisy tails.

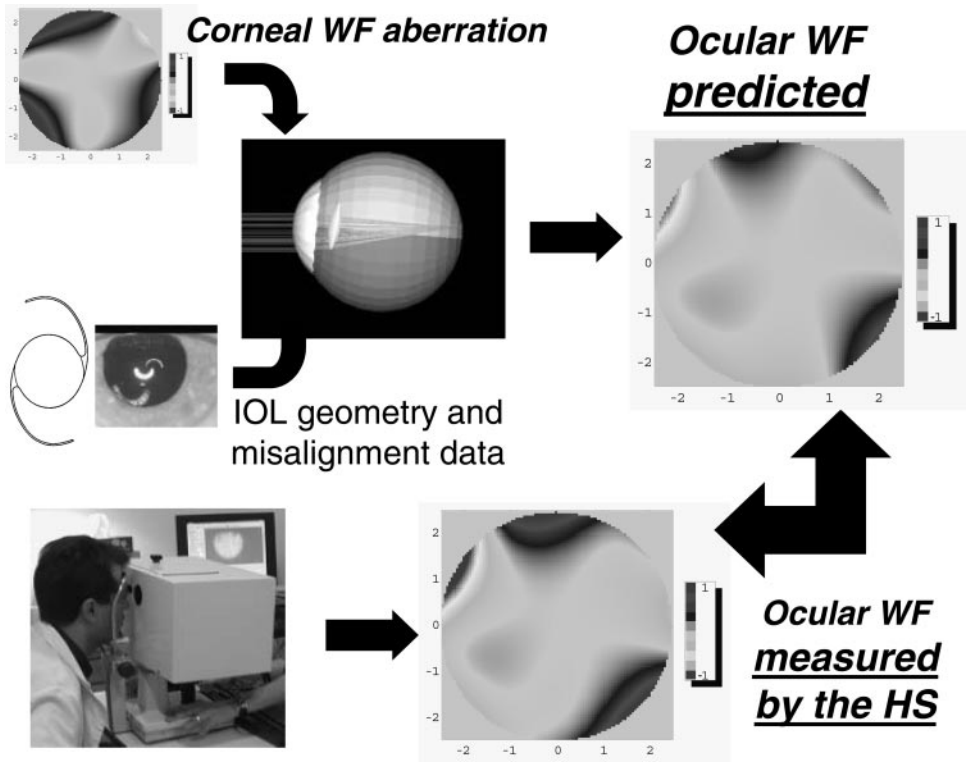

FIGURE 3. Schematic diagram of the customized modeling for virtual optical surgery. The predicted wavefront aberration (WF) obtained by the calculation with actual experimental data is compared with the measured WF.

Downloaded From: http://jov.arvojournals.org/ on 07/24/2015

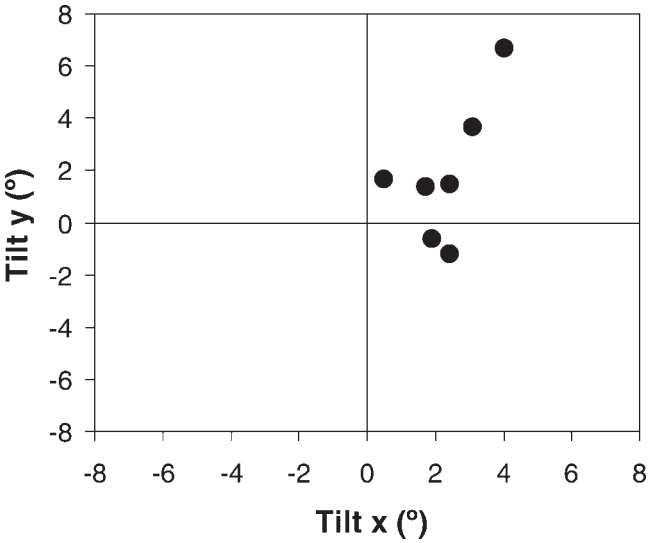

FIGURE 4. IOL tilt with respect to the pupillary axis measured with the Purkinje meter.

RESULTS

IOL Misalignments

IOL tilt with respect to the pupillary axis and IOL decentration were measured as described and are shown in Figures 4 and 5, respectively. A temporal IOL tilt (positive sign) means that the optical axis of the IOL is tilted toward the temporal side of the pupillary axis in object space. IOL tilt was, on average, 2.2° temporal (SD 1.1°) in the horizontal direction and 2.2° superior (SD 2.6°) in the vertical direction. Figure 5 indicates a temporal tendency (positive sign) for decentration, except in one subject who had a considerable nasal decentration of 0.4 mm. The range of decentration on the temporal side was from 0.06 to 0.2 mm. In the vertical direction, there was one subject with a considerable inferior decentration of −0.65 mm, whereas the rest of the subjects showed a small degree of decentration −0.07 mm (inferior) to 0.17 mm (superior).

Figure 6 shows an example of one image taken with our instrument where the three reflections (Purkinje images of the semi circular targets) can clearly be seen and identified in the picture. In the case of subjects with a pupil size large enough, it was also possible to visualize the IOL edges and therefore to check the values of IOL decentrations we measured. This was an independent procedure to evaluate our approach to estimate IOL location after surgery.

Comparison of Predicted and Measured Aberrations

The predicted (by modeling) and directly measured SA correspond well. Figure 7 shows how these two values are related for all subjects. As expected, those eyes implanted with the CeeOn TM IOL had a higher value of SA (average 0.15 μm; SD 0.06) than those implanted with a Tecnis TM lens (average 0.00, SD 0.04). Figure 8 shows all the Zernike terms (excluding tilt and defocus) of the ocular wavefront aberration we measured and the ocular aberration we calculated with the modeling for all subjects. These results provide an indication of the accuracy of the virtual surgery procedure and how well the actual aberrations can be predicted. Figure 3 shows an example for one subject of how similar the predicted and measured wavefront maps are. These positive results allow us to extend the procedure to predict the behavior of different IOLs under a variety of possible situations created by actual surgical procedures.

Predictions of Performance: Misalignments and Defocus

In particular, we use the procedure to evaluate how tolerant to decentrations SA correcting IOLs are in comparison to standard spherical IOLs. The parameter defined in equation 1 (improvement fraction) was calculated at 6 cyc/deg for each subject as a function of orthogonal decentration and tilt directions. Figures 9 to 12 show the average and standard deviation of the improvement fraction for various amounts of IOL decentration and tilt. The regions where this fraction is positive indicate an improvement in optical quality for the aspheric IOL with respect to the spherical IOL, whereas a region of negative fraction indicates a better optical performance for the conventional spherical IOL than for the aspheric design. The thick lines in the lower part of each plot are the projections of the positive regions. They provide tolerances to misalignments for each case. The data points are the actual values of decentration and tilt measured for each patient in the study.

In a similar way we compare the performance of both IOLs with respect to depth of focus. Figure 13a shows depth-of-focus average values (obtained by equation 2) for both the Tecnis TM and for the CeeOn TM lenses. These results should be compared with those in Figure 13b: the experimental data obtained using adaptive optics to simulate vision with and without correction of SA.[9]

DISCUSSION

The use of new technology in wave-front sensing and a better understanding of the nature of the aberration in the normal aging eye has enabled the development of aspheric IOLs that are a real alternative to conventional designs for use in cataract surgery. However, some questions may arise with the use of these new lenses, and there is also a clear need for more adequate assessment techniques. The problem with IOL tolerances to misalignments is an example of this situation. In this article, we have presented advanced instruments and compu-

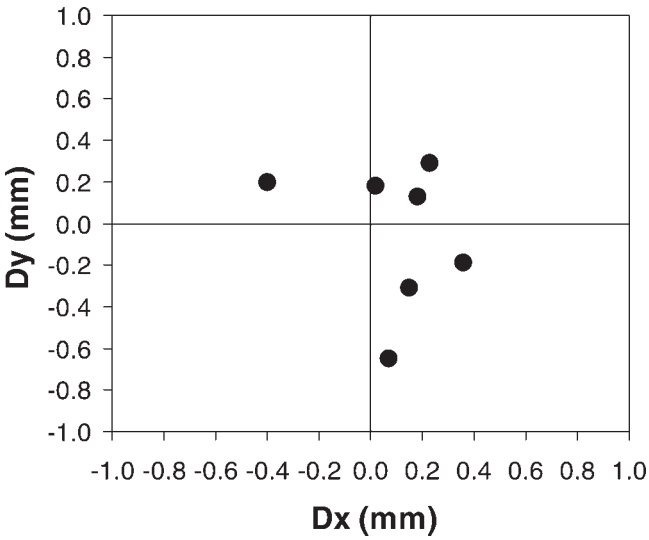

FIGURE 5. IOL decentration with respect to the pupil center measured with the Purkinje meter.

Downloaded From: http://jov.arvojournals.org/ on 07/24/2015

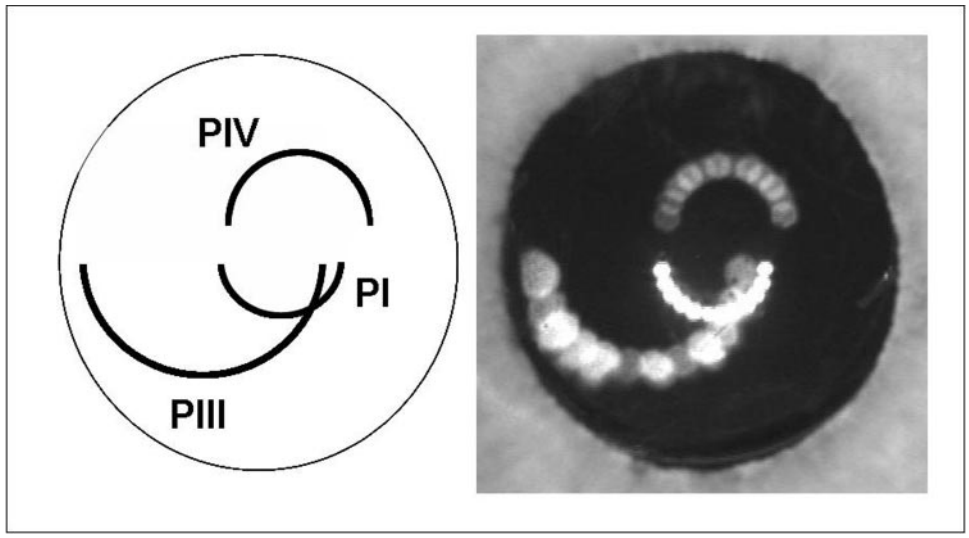

FIGURE 6. Example of one of the images recorded with the Purkinje meter. The first, third, and fourth Purkinje images of the semicircular target are clearly seen.

tational tools to address this question in a unique way. This is what we refer to as virtual surgery, a powerful experimental and computational procedure that allows us to evaluate the optical performance of current and future generations of aberration-controlling IOLs.

Our first goal was to verify that the aspheric IOLs were indeed correcting for the corneal SA. Figure 7 showed that the corneal SA was actually well balanced by the intraocular lens's SA, in agreement with clinical studies. This would be enough if the eye after surgery were a perfectly aligned optical instrument, free from other aberrations, but of course this is not the real case, and simple modeling as performed in the past is not adequate to predict correctly the performance of IOLs in real eyes. A customized and realistic modeling of the pseudophakic eye is needed To build up our customized computational model we need to know the cornea, which is approximated by a one-surface model constructed using real data derived from corneal topography, the specific IOL design and also how tilted and decentrated the IOL was after surgery, together with other ocular biometric data. The customized modeling produced data of the eye's aberrations that were extremely well correlated with those actually measured. This is considered a validation of our procedure that permitted its application to study any type of IOL design and different structural configurations. In others words, we were able to perform what we called a customized virtual surgery for each particular cataract patient.

To compare the performance of both IOL models (aspheric and spherical) we defined the improved fraction in terms of the radially averaged MTF, and we computed it as a function of lens decentration and tilt in orthogonal directions. Our results showed nonsymmetric limits for the positive improvement fraction regions (where the performance of the aspheric lens is better than that of the conventional spherically surfaced IOL). It is important to note that the zero point for decentrations in these calculations was the pupil center, and the axis we used to calculate the aberrations was the line of sight. It is well known that the pupillary axis and the line of sight are nonparallel axes.[18,27] The pupillary axis tends to be temporal with respect to the line of sight (in object space). Therefore, the corneal apex tends to be on the temporal side with respect to the interception point between the cornea and the line of sight. Therefore, it is possible that a temporal shift of the IOL

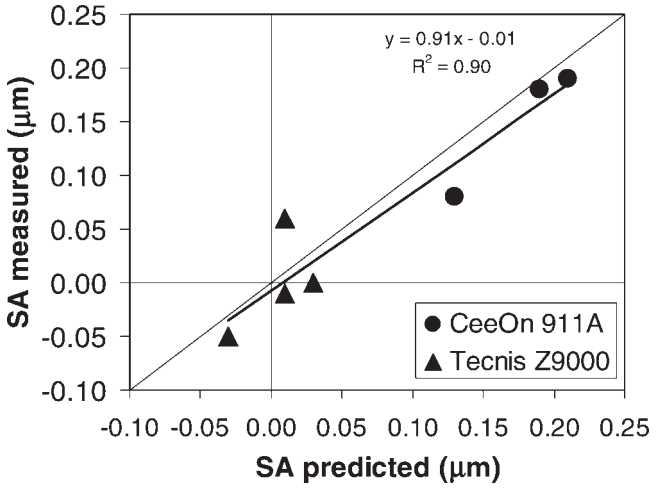

FIGURE 7. Ocular SA (Z, 4.0) predicted by our procedure as function of ocular SA (Z 4.0) measured by our Hartmann-Shack wavefront sensor.

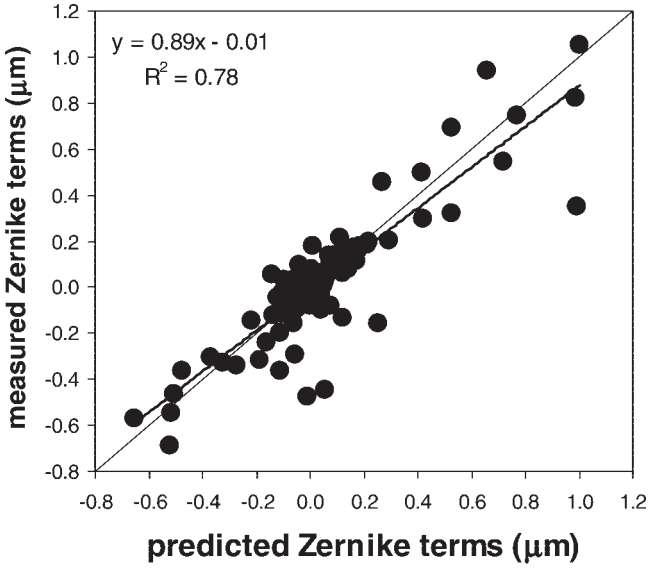

FIGURE 8. All Zernike terms of the wavefront aberration predicted by our model as a function of the Zernike terms directly measured. The high degree of correlation is an indication of the potential of the modeling procedure.

Downloaded From: http://jov.arvojournals.org/ on 07/24/2015

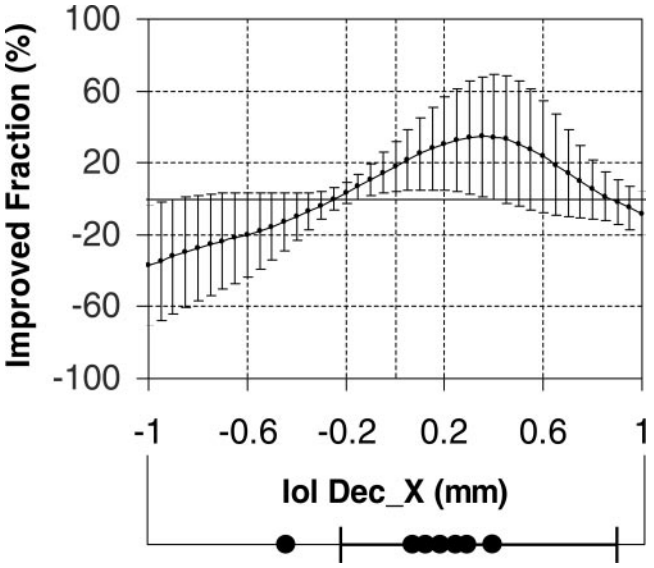

FIGURE 9. Radial MTF improved fraction at 6 cyc/deg as a function of IOL decentration in the *x* direction. Error bars: SD.

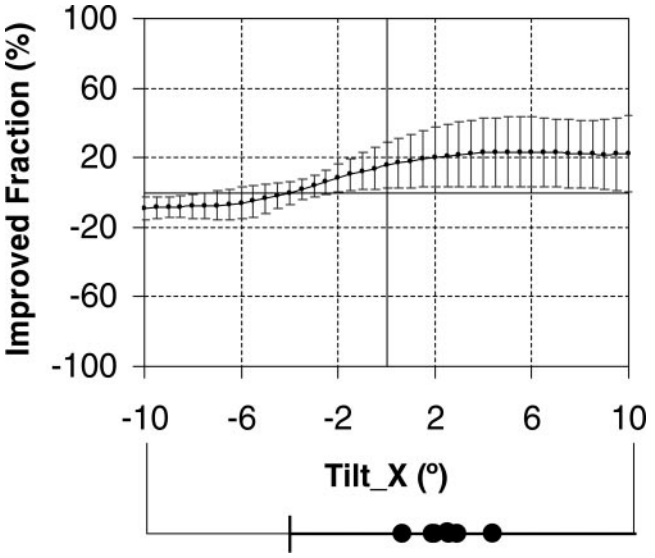

FIGURE 11. Radial MTF improved fraction at 6 cyc/deg as a function of IOL tilt in the *x* direction. Error bars, SD.

may have a realignment effect between cornea and IOL that slightly improves the overall optical quality. A similar effect was found when the IOL was tilted in the temporal direction. However, the vertical decentration and vertical tilt were more symmetric. This is also in agreement with the classic physiological optics literature, in which it was established that the main foveal misalignment with respect to the optical axis was temporal, therefore horizontal.

It is interesting to note that IOL decentration has more effect on optical performance than IOL tilt. Therefore, decentration of aspheric lenses is more critical than tilt. This is consistent with previous studies,[28] and it may suggest that surgeons should avoid decentration where possible when implanting aspheric IOLs. It should also be mentioned that it is possible to find nonlinear effects due to the combination of both parameters in the case of very strong tilts and decentrations.

These results also may suggest that the tolerances we found were large enough to provide an optical benefit from an aspherically designed IOL within the limits imposed by modern cataract surgery. Only one of the tested subjects had a large enough decentration in the nasal direction to reduce the optical benefit of balancing the corneal SA. For this subject, correcting SA was not enough to achieve better optical quality with the aspheric IOL.

It is also important to note that these figures (Figs. 9–12) are only the tolerances in two orthogonal directions, *x* and *y*. Actually every lens is decentered in a different direction. This direction is geometrically decomposed in two components along the *x* and *y* axis, which is not an exact solution. However, it is useful to understand what happens in these two decentration directions, because it provides us with a full understanding of the most structurally different directions.

Concerning depth of focus, it is worthwhile to mention that the average levels that we obtained had a very similar tendency

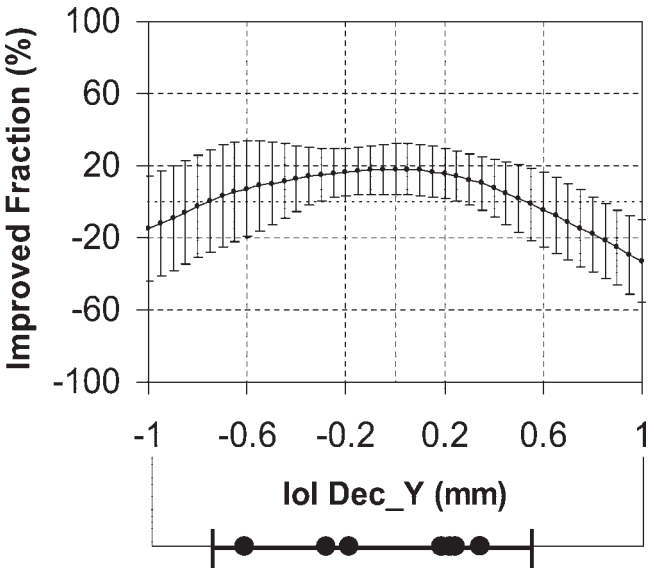

FIGURE 10. Radial MTF improved fraction at 6 cyc/deg as a function of IOL decentration in the *y* direction. Error bars, SD.

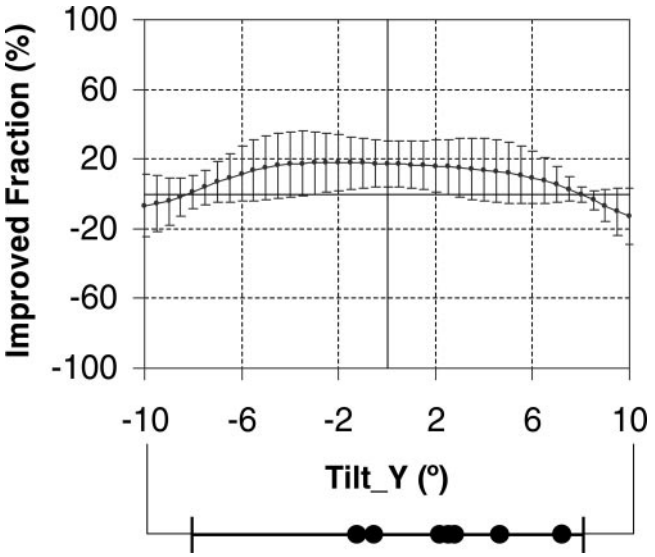

FIGURE 12. Radial MTF improved fraction at 6 cyc/deg as a function of IOL tilt in the *y* direction. Error bars, SD.

Downloaded From: http://jov.arvojournals.org/ on 07/24/2015

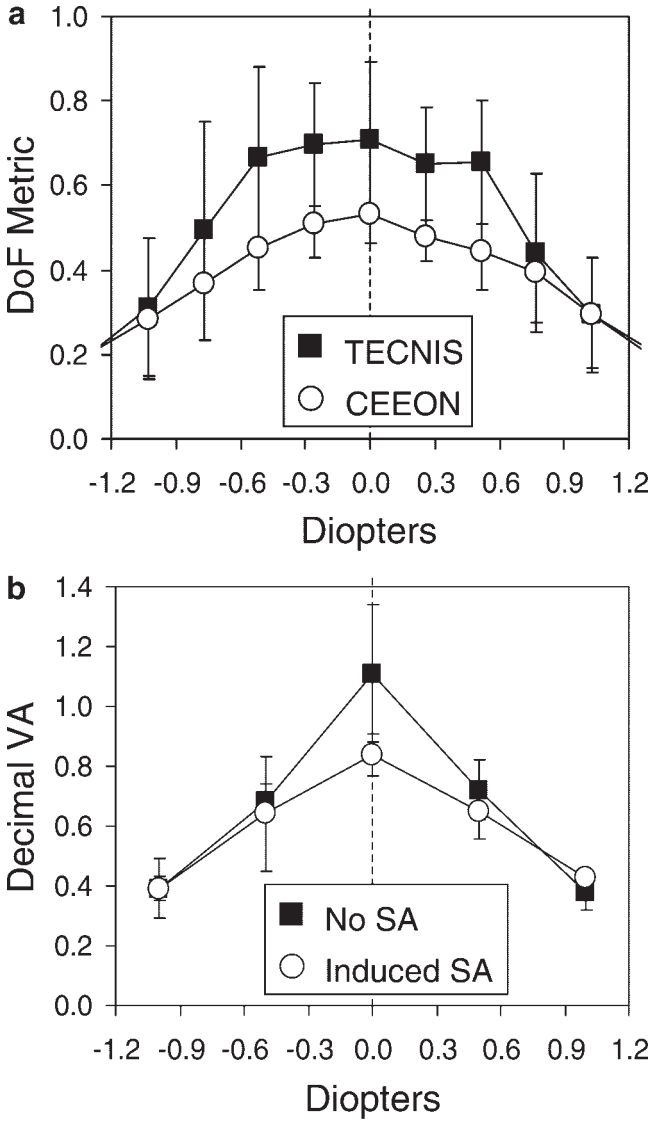

FIGURE 13. (**a**) Square PSF versus defocus for Tecnis TM and CeeOn TM IOLs. (**b**) Decimal visual acuity versus defocus in patients with induced SA and corrected SA.

toward those averages found by using adaptive optics in laboratory conditions (Fig. 13). This result confirms the validity of our approach. It also may suggest that, on average, tolerances to depth of focus are not very critical for the IOLs correcting SA, although interindividual variations were observed and further statistically meaningful studies are necessary to validate this point.

Another potential limitation to our study is its monochromatic character. Although this is an important aspect, we believe that the current monochromatic analysis provides enough important and valid information. The extension of the procedure to consider white light is possible, however, and will be the subject of further research.

We have addressed for the first time, as far as we know, the problem of IOL misalignments with a completely realistic approach. We developed instrumentation for measuring different ocular parameters and built a complete and realistic computational pseudophakic eye model, from which we can extract multiple reliable predictions. With the recent increase in the use of aspheric IOLs, extensive research is expected to evaluate potential surgical outcomes. This procedure will also be quite useful for the design and evaluation of other types of IOLs and for the understanding of different optical and visual outputs.

References

1. Artal P, Guirao A, Berrio E, Williams DR. Compensation of corneal aberrations by the internal optics in the human eye. *J Vision.* 2001;1:1–8.
2. Artal P, Benito A, Tabernero J. The human eye is an example of robust optical design. *J Vision* 2006;6:1–7.
3. Artal P, Ferro M, Miranda I, Navarro R. Effects of aging in retinal image quality. *J Opt Soc Am A.* 1993;10:1656–1662.
4. Guirao A, González C, Redondo M, Geraghty E, Norrby S, Artal P. Average optical performance of the human eye as a function of age in a normal population. *Invest Ophthalmol Vis Sci.* 1999;40:203–213.
5. Artal P, Berrio E, Guirao A, Piers P. Contribution of the cornea and internal surfaces to the change of ocular aberrations with age. *J Opt Soc Am A.* 2002;19:137–143.
6. Guirao A, Redondo M, Geraghty E, Piers P, Norrby S, Artal P. Corneal optical aberrations and retinal image quality in patients in whom monofocal intraocular lenses were implanted. *Arch Ophthalmol* 2002;120:1143–1151.
7. Holladay JT, Piers PA, Koranyi G, van der Mooren M, Norrby NE. A new intraocular lens design to reduce spherical aberration of pseudophakic eyes. *J Refract Surg.* 2002;18:683–691.
8. Guirao A, Redondo M, Artal P. Optical aberrations of the human cornea as a function of age. *J Opt Soc Am A.* 2000;17:1697–1702.
9. Piers PA, Fernandez EJ, Manzanera S, Norrby S, Artal P. Adaptive optics simulation of intraocular lenses with modified spherical aberration. *Invest Ophthalmol Vis Sci.* 2004;45:4601–4610.
10. Mester U, Dillinger P, Anterist N. Impact of a modified optic design on visual function: clinical comparative study. *J Cataract Refract Surg.* 2003;29:652–660.
11. Bellucci R, Scialdone A, Buratto L, et al. Visual acuity and contrast sensitivity comparison between Tecnis and AcrySof SA60AT intraocular lenses: a multicenter randomized study. *J Cataract Refract Surg.* 2005;31:712–717.
12. Hayashi H, Hayashi K, Nakao F, Hayashi F. Intraocular lens tilt and decentration, anterior chamber depth, and refractive error after trans-scleral suture fixation surgery. *Ophthalmology.* 1999;106:878–882.
13. Hayashi K, Hayashi H, Nakao F, Hayashi F. Correlation between pupillary size and intraocular lens decentration and visual acuity of a zonal-progressive multifocal lens and a monofocal lens. *Ophthalmology* 2001;108:2011–2017.
14. Oshika T, Kawana K, Hiraoka T, Kaji Y, Kiuchi T. Ocular higher-order wavefront aberration caused by major tilting of intraocular lens. *Am J Ophthalmol.* 2005;140:744–746.
15. Dubbelman M, van der Heijde GL, Weeber HA. The thickness of the aging human lens obtained from corrected Scheimpflug images. *Optom Vis Sci.* 2001;78:411–416.
16. Dubbelman M, Weeber HA, van der Heijde GL, Volker-Dieben HJ. Radius and asphericity of the posterior corneal surface determined by corrected Scheimpflug photography. *Acta Ophthalmol Scand.* 2002;80:379–383.
17. Cook CA, Koretz JF. Methods to obtain quantitative parametric descriptions of the optical surfaces of the human crystalline lens from Scheimpflug slit-lamp images. I. Image processing methods. *J Opt Soc Am A* 1998;15:1473–1485.
18. Le Grand Y, El Hage SG. *Physiological Optics.* Berlin: Springer-Verlag; 1980;13.
19. Phillips P, Pérez-Emmanueilli J, Rosskothen HD, Koester CJ. Measurement of intraocular lens decentration and tilt in vivo. *J Cataract Refract Surg.* 1988;14:129–135.
20. Auran JD, Koester CJ, Donn A. In vivo measurement of posterior chamber intraocular lens decentration and tilt. *Arch Ophthalmol.* 1990;108:75–79.
21. Barry JC, Branman K, Dunne MCM. Catoptric properties of eyes with misaligned surfaces studied by exact ray tracing. *Invest Ophthalmol Vis Sci.* 1997;38:1476–1484.

Downloaded From: http://jov.arvojournals.org/ on 07/24/2015

22. Barry JC, Dunne MCM, Kirschkamp T. Phakometric measurement of ocular surface radius of curvature and alignment: evaluation of method with physical model eyes. *Ophthalmic Physiol Opt*. 2001;21:450–460.
23. Kirschkamp T, Dunne MCM, Barry JC. Phakometric measurement of ocular surface radii of curvature axial separation and alignment in relaxed and accommodated human eyes. *Opthalmic Physiol Opt*. 2004;24:65–73.
24. Guirao A, Artal P. Corneal wave aberration from videokeratography: accuracy and limitations of the procedure. *J Opt Soc Am A.* 2000;17:955–965.
25. Prieto PM, Vargas-Martín F, Goelz S, Artal P. Analysis of the performance of the Hartmann-Shack sensor in the human eye. *J Opt Soc Am A*. 2000;17:1388–1398.
26. Guyton DL, Uozato H, Wisnicki HJ. Rapid determination of intraocular lens tilt and decentration through the undilated pupil. *Ophthalmology*. 1990;97:1259–1264.
27. Atchison DA, Smith G. *Optics of the Human Eye.* Butterworth-Heinemann; 2000.
28. Atchison DA. Design of aspheric intraocular lenses. *Ophthalmic Physiol Opt*. 1991;11:137–146.

Downloaded From: http://jov.arvojournals.org/ on 07/24/2015